GEOLOGY OF THE ZHURONG LANDING SITE AND ACCESS TO THE DEEP BIOSPHERE ON MARS.

B. Ye[1], Y. Qian[2]. L. Xiao[2], J. R. Michalski[1], Y.L. Li[1], B. Wu[3], L. Qiao[4], [1]Dept. of Earth Sciences and Laboratory for Space Research, University of Hong Kong, Hong Kong SAR, China (binlongy@hku.hk), [2]State Key Laboratory of Geological Processes and Mineral Resources, School of Earth Sciences, China University of Geosciences, Wuhan, China, [3]Dept. of Land Surveying and Geo-Informatics, The Hong Kong Polytechnic University, Kowloon, Hong Kong SAR, China, [4]Shandong Key Laboratory of Optical Astronomy and Solar-Terrestrial Environment, School of Space Science and Physics, Shandong University, Weihai, China.

Introduction: China's Mars probe, named Tianwen-1, has arrived at the Red Planet. Different from previously Mars explorations, it has been the first Mars mission that integrates orbiting, landing, and roving [1-3]. On May 15, 2021, Tianwen-1's rover Zhurong, landed successfully in southern Utopia Planitia in the northern plain of Mars. The terrain is topographically smooth and low in elevation. The landing region has experienced complex geological evolution, with long-term volcanic, fluvial, aeolian, periglacial and glacial modifications [4-8]. Here, we analyze the surrounding environments of the landing site and consider potential mud volcanoes with directly accessible to Zhurong rover [9] have potential astrobiology implications.

Methods: Context Imager (CTX, 6m/pixel) corrected mosaics and High-Resolution Imaging Science Experiment (HiRISE, 0.3 m/pixel) data were used to map geomorphological features of the Zhurong landing site. Mars Orbiter Laser Altimeter (MOLA) provides quantitative topographic analysis at 463 m/pixel. We also use the Ames Stereo Pipeline (ASP) to generate high-resolution CTX and HiRISE digital elevation models.

Results: High-resolution imagery and topography data are produced to characterize the morphology features of Zhurong landing site and map their distribution, including troughs, raised ridges, pitted cones, mesas, and crater ejecta (Fig. 1).

Pitted cones are the most prominent and abundant landforms in the study region, with >4000 identified features. Relative to the adjacent ground, the surface texture of these cones is commonly smooth, and there is a central depression on the top (Fig. 1a). In local areas, some cones appear in chains (Fig. 1b), and some are distributed in clusters rather than a sporadical manner (Fig. 1c). We also measured the height and basal width of pitted cones to constrain their origin [9].

Linear or polygonal troughs (Fig. 1d) are widespread in the northern part of the mapping region (Fig. 1i). Throughs' length varies from 0.4 – 50 km and the width ranges from ~100 m to 1000 m. These troughs might form through tectonic uplift and extension of the Utopia basin after the sublimation of the ice-rich substrate [10]. The most interesting aspects are the geospatial relationships between these troughs and pitted cones: The northeast mapping region is dominated by troughs while the pitted cones are mainly distributed in the southwest. Troughs are commonly found in the central Utopia basin in the north, and only a few spots show pitted cones. Fortunately, the rover landed near the boundary of a geomorphological transition from trough forming to cone-forming processes.

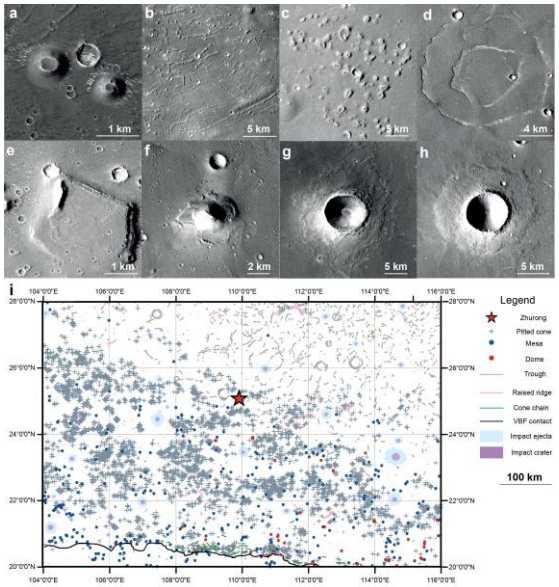

Figure 1. CTX and HiRISE images show varied landforms near the Zhurong landing site: (a) pitted cones, (b) pitted cone chains, (c) cone clusters, (d) troughs, (e) mesas (105.5◦E, 22.3◦N; CTX), (f) domes, (g) rampart craters, (h) pancake-like ejecta. (i) The distribution of geomorphological features in the study region [9].

Discussion: A variety of formation mechanisms of pitted cones on Mars have been proposed, including interpretations as mud volcanoes [11, 12], cinder/scoria cones [13], tuff cones/rings [14], rootless cones [15], and pingos [16], which have different implications.

Morphologically, these pitted cones are unlike pingos elsewhere on Mars, which have flat-topped mounds with meter-scale polygonal troughs or cracks fracturing surface textures that otherwise resemble that of nearby surrounding terrain. Rootless cones are generally associated with raised rims along the edges of

summit pits, which is not the case here. Pitted cones here are also a few orders of magnitude larger than the rootless cones. The size of scoria/cinder cones and tuff rings/cones in this study are significantly smaller than those on Earth and Mars elsewhere, they, however, show similar relationships when comparing height/basal aspect ratios. In addition, the spatial correlation between pitted cones and troughs could partly be explained by the latitude-dependent water-ice abundance, thickness, or possibility of melting. Though hydrovolcanic features such as maars might be affected by latitude-depenent permafrost, scoria and cinder cones would be less likely to show variations in morphology and abundance with latitude. It is possible that once the permafrost layer is formed, it stops subsurface fluidized sediments and gas from upwelling to form mud volcanoes (Fig. 2). The geologic context suggests this region could be the depocenter of the Hesperian catastrophic flood, which would contain an enormous reservoir of volatile rich mud or slurry around the Utopia basin, providing favorable conditions for sediment upwelling. Therefore, those lines of evidence supports that mud volcanoes are the most plausible scenario.

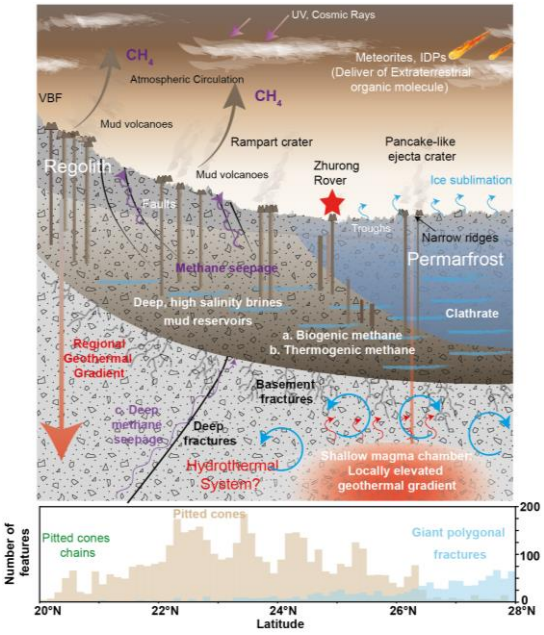

Figure 2. A schematic cross-section shows ice, mud, and volcanism interaction in the past of the Zhurong landing region in Utopia Planitia.

Mud Volcano as A Natural Deep Drill: Unlike cold and oxidized surface, the subsurface of Mars could provide energy, and liquid for life emerging and survival, which is a plausible environment to search for biosignatures and evidence of life [17]. The question is how could we have access to these deep subsurface materials? Radar provides information about 1 km depth, but with ambiguous interpretations. Rovers can detect the mineralogy and chemistry of a few dozen cm of surface with small abrade tools. With the current technology, although it might be possible drill as deep as 100 m, but the expense be prohibitive [18].

Mud volcanoes on Earth, generally expel subsurface materials from several km deep, including fluidized sediments and gas [19]. Like impact craters, which are natural probes into the subsurface, mud volcanoes could also provide invaluable access to uplifted subsurface materials. However, the fine-grained sediments expelled by mud volcanoes would not be shocked, melted or fragemented, and would provide unique access to deep sediments, which on Earth can contain significant organic materials. Zhurong is equipped with many payloads, including a terrain camera, multispectral cameras, a Mars surface composition detector [1, 3]. For the Navigation Camera and Multispectral Camera, it can provide some information on morphology and mineralogy. The MarSCoDe consists of two parts, LIBS and VNIR spectroscopy, which can provide in-situ mineralogy and chemical data. The penetrating radar has two channels that can penetrate 10 m and 100 m, respectively. It will offer some new insights into subsurface sedimentary structures and ice at subtitle scales.

Acknowledgments: All data used in this paper are available in NASA Planetary Data System (pds.jpl.nasa.gov). CTX mosaic data are available on this website (http://murray-lab.caltech.edu/CTX/).

References: [1] Zou, Y., et al. (2021) *Adv. in Space Research*, 67(2): p. 812-823. [2] Wan, W., et al. (2020) *Nature Astronomy*, 4(7): p. 721-721. [3] Li, C., et al. (2021) *Space Sci. Rev.*, 217(4): p. 1-24. [4] Wu, X., et al. (2021) *Icarus*, 370: p. 114657. [5] Zhao, J., et al. (2021) *GRL*, 48(20). [6] Wu, B., et al. (2021) *Earth and Space Sci*., [7] Liu, J., et al. (2021) *Nature Astronomy*, p. 1-7. [8] Ivanov, M., et al. (2015) *Icarus*, 248: p. 383-391. [9] Ye, B., et al. (2021) *EPSL*, 2021. 576: p. 117199. [10] Hiesinger, H. and Head J.W. (2000) *JGR-Planets*, 105(E5): p. 11999-12022. [11] Brož, P., et al. (2019) *JGR-Planets*, 124(3): p. 703-720. [12] Hemmi, R. and Miyamoto H. (2017) *Progress in Earth and Planetary Science*, 4(1). [13] Brož, P., et al. (2015) *JGR-Planets*, 120(9): p. 1512-1527. [14] Brož, P. and E. Hauber E. (2013) *JGR-Planets*, 118(8): p. 1656-1675. [15] Noguchi, R. and Kurita K. (2015) *Planetary and Space Science*, 2015. 111: p. 44-54. [16] de Pablo, M.Á. and Komatsu G. (2009) *Icarus*, 2009. 199(1): p. 49-74. [17] Michalski, J.R., et al. (2018) *Nature Geoscience*, 11(1): p. 21-26. [18] Stamenković, V., et al. (2019) *Nature Astronomy*, 3(2): p. 116-120. [19] Mazzini A. and Etiope G. (2017) *Earth-Science Reviews*, 168: p. 81-112.